CFD MODELING OF SOOT INDUCED RADIATION IN THE EXHAUST PLUME OF ROCKET ENGINES

S. Karl, T. Ecker, T. Bykerk

German Aerospace Center, DLR
Institute of Aerodynamics and Flow Technology
Göttingen, Germany

S. Choi, J. Kim

Korea Aerospace Research Institute
Daejeon, Republic of Korea

ABSTRACT

This paper presents a computational methodology to quantify plume radiation caused by soot particles in rocket exhaust plumes. A Photon-Monte-Carlo-Method is used to solve the radiative transfer equation. This approach accounts for self-absorption in the exhaust gas which is significant as the plume is close to the optically thick limit for full scale launcher configurations. The radiative properties such as the absorption coefficient (inverse mean free path of the photons) and the emissivity (emitted radiative power per volume and direction) are derived from estimates of the soot mass fraction and particle size. The plume shape and thermodynamic properties are taken from classical CFD analyses. The method is calibrated and assessed based on available flight data for a kerosene-fueled rocket engine at different altitudes. Strong agreement with flight data was achieved by using estimates for soot properties which are consistent with the current literature.

Index Terms— launch vehicles, thermal loads, CFD, radiation

1. INTRODUCTION

Hydro-carbon fueled rocket engines produce soot which is also present in the exhaust jet. The quantification of the soot concentration and particle size is extremely difficult and by now only order of magnitude estimates exist. Nevertheless, the prediction of soot emissions is of technical importance. Especially at higher altitudes, they may have adverse environmental effects and contribute to radiative forcing and, hence, global warming. Further, soot-induced radiation can cause significant heat loads in the vicinity of the launcher base which may reach a similar order of magnitude as convective heat loads. This imposes additional demands on the design of thermal protection systems. This paper presents a computational methodology to quantify plume radiation caused by soot particles. A Photon-Monte-Carlo-Method is used to solve the radiative transfer equation. This approach accounts for self-absorption in the exhaust gas which is significant as the plume is close to the optically thick limit for full scale launcher configurations. The radiative properties such as the absorption coefficient (inverse mean free path of the photons) and the emissivity (emitted radiative power per volume and direction) are derived from estimates of the soot mass fraction and particle size. The plume shape and thermodynamic properties are taken from classical CFD analyses. The results are assessed based in available flight data of the TLV launcher configuration [1] on 3 trajectory points covering an altitude range between 5 km and 20 km. The presented methodology can be used to estimate radiative heat loads with known particle sizes and number densities. Or, inversely, to estimate particle properties from known radiation measurements.

2. MONTE-CARLO-METHOD FOR RADIATIVE TRANSFER

The Monte-Carlo-Method aims at the direct simulation of the physical process of the radiation propagation. It uses a computational grid which is composed of a large number of control volumes (similar to a CFD grid). The energy which is emitted in each control volume is distributed to a large number of independent computational particles or photons. Hence, the radiative energy is treated as a distributed rather than a continuous quantity. The photons are then emitted to random directions and their flight path through the computational domain is traced. Hence, the implementation of a computationally efficient ray-tracer is the most important feature of a Monte-Carlo method. Our algorithm uses a finite-element approach in which the control volumes are converted to unit shape by shape functions and the same shape function is then used to convert the flight direction into unit space which makes it easy to determine at which face the photon leaves the volume. The neighboring volume is then identified by a pre-computed lookup table. Monte Carlo Methods enable computations in complex geometries, the application of unstructured highly adaptive grids and spectrally resolved transfer computations. Nevertheless, they come with the disadvantage od statistical noise in the solution and they suffer from a high numerical complexity (large increase of computational effort due to grid refinement).

A schematic algorithm of the applied Monte-Carlo method

is composed from the following steps:

1. The total radiative power being emitted in a control volume or grid cell is distributed to a fixed number of computational photons. The number of these photons is usually related to the amount of emitted energy which introduces a highly adaptive solution scheme. Spectral resolution can be introduced by assigning wavelength-specific values to the particles.
2. Each computational photon is emitted to a random direction. For volume cells, a uniform distribution is chosen. For emission from walls a specific probability density function for the emission direction is selected (most often a Lambert-cosine distribution).
3. The path of each photon is traced through the computational domain.
4. Along the flight path, the optical distance which is passed through py a particle, L, is integrated ($L = \int \alpha \mathrm{d}s$).
5. If this optical distance exceeds a random absorption limit, the energy carried by the particle is assigned to the respective control volume.
6. If the particle is hits a boundary it is either lost (ambient), reflected (symmetry) or absorbed and re-emitted (solid wall).

When a photon is absorbed somewhere in the computational domain, its entire energy is assigned to the respective computational cell and the photon is lost. To decide whether a photon is absorbed after a certain flight distance or not, a uniformly distributed random number, Rs, is assigned to each photon. The absorption criterion is:

$$\int \alpha \mathrm{d}s \geq -\ln\left(1 - R_s\right) \tag{1}$$

The left hand side of this expression is provided ray tracing of the photon flight path through the computational domain. The right hand side transforms a uniformly distributed random number, R_s, to the physical absorption distribution given by Beer's law for the radiative intensity, I. This can be obtained by the solution of the 1D radiative transfer equation assuming no emission:

$$\frac{I}{I_0} = \exp\left(-\int \alpha \mathrm{d}s\right) \tag{2}$$

Eq. 1 can be obtained by assuming that the probability of the absorption of a computational particle, P, is described by a uniformly distributed random number, R_s, and replacing the intensity fraction I/I_0 with eq. 2:

$$P = R_s = 1 - \frac{I}{I_0} = 1 - \exp\left(-\int \alpha \mathrm{d}s\right) \tag{3}$$

When a photon hits a wall it is absorbed and re-emitted. The energy of the re-emitted photon is decreased according to the absorption coefficient of the wall:

$$e_{\mathrm{emitted}} = (1 - \alpha_{\mathrm{wall}}) e_{\mathrm{incident}} \tag{4}$$

The energy difference is added to the radiative wall heat flux.

3. TEST LAUNCH VEHICLE

The computational methodology for the radiative heat flux is applied to the Test Launch Vehicle (TLV) which is part of the development program of the Korean Space Launch Vehicle II (KSLVII). Its main purpose is to demonstrate and test the kerosene fueled main engine of the KSLV with about 75 tons of thrust. The TLV is composed of two stages. The first stage has 15.37 m of length and 2.6 m of diameter. It has a single main engine with exhaust plumes from the thrust nozzle and the gas generator exit. A schematic of the TLV vehicle is shown in figure 3. Comprehensive analysis of the TLV aerothermal environment including flight test data for convective and radiative heat transfer is provided by Kim [1].

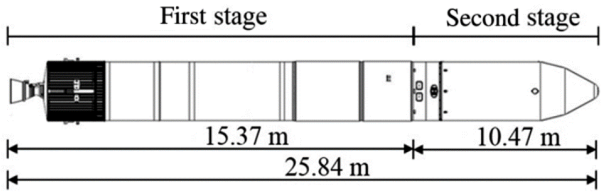

Fig. 1. Schematic of the TLV [1]

4. BASELINE CFD

The baseline CFD simulations for this study were done with the DLR TAU Code [3] which is a second order finite-volume solver for the Navier-Stokes equations. The present computations are performed with an AUSMDV upwind solver for the inviscid fluxes along with the Menter-SST turbulence model. The flow was treated as a reacting mixture of thermally perfect gases with 11 species in total. The exit conditions of the main engine were obtained by numerical simulation of the nozzle flow in chemical non-equilibrium using the hydrogen/oxygen/carbon-oxide reaction mechanism of Ecker [4]. The exit conditions of the gas generator were estimated using the CEA equilibrium solver [5]. The chemical interaction of the man engine and gas generator exhaust with the ambient air was modeled with the Westbrook-Dryer two-step global Mechanism [6]. The TLV trajectory points which are considered in this study are summarized in table 1. A qualitative view of the flowfield in the vicinity of the base is given in figure 4.

Table 1. Trajectory points

Name	Mach	AoA	p_∞	T_∞
TP1	0.7	5 deg	54 kPa	260 K
TP2	1.2	5 deg	27 kPa	230 K
TP3	2.1	5 deg	5.5 kPa	208 K

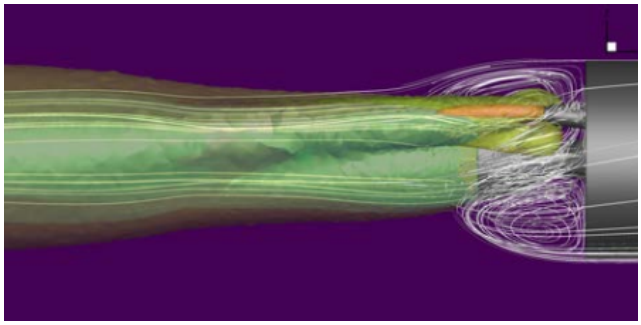

Fig. 2. CFD flow field in the vicinity of the base for TP1

5. ESTIMATE OF THE RADIATIVE PROPERTIES OF THE EXHAUST GAS

Literature data for soot emissions of liquid kerosene-oxygen engines [7, 8, 9, 10] suggest an average particle size of 1 μm and a range of average mass fraction of black carbon in the exhaust gas of 0.2-0.4 %. These data are either obtained from numerical analyses [7], optical measurements in exhaust plumes [8] or global data bases used for the quantification of the atmospheric impact of launch emissions [10, 9]. For the present analyses we used a constant soot mass fraction of 0.3 % in the exhaust gas and an average particle diameter of 1 μm.

The properties of the exhaust which are needed to solve the radiative transfer problem are the local absorption coefficient, α, and the emissivity, e. The simple model of a cloud of spherical particles was used to estimate these properties.

The absorption coefficient is the inverse mean free path of the photons (λ). It is estimated from the number density of particles, N, and the effective particle cross-section as:

$$\alpha = \frac{1}{\lambda} = \frac{\pi}{4} d^2 N \tag{5}$$

The emissivity is the amount of emitted radiative energy per unit volume and per unit solid angle. It is estimated using the Stefan-Boltzmann law and the total particle surface per unit volume:

$$e = \frac{1}{4\pi} \sigma T^4 A = \frac{1}{4} \sigma T^4 d^2 N \tag{6}$$

The number density of particles in the exhaust is:

$$N = \frac{Y_e \rho_e}{\rho_{BC}} \frac{8\pi}{d^3} \tag{7}$$

where Y_e is the mass fraction of black carbon in the exhaust, ρ_{BC} is the density of solid carbon and ρ_e is the local partial density of the exhaust gas.

Figure 5 shows a sensitivity analysis for the radiative intensity, I, at the end of a 15 m long exhaust plume at typical conditions with a density of 0.1 $\mathrm{kg/m^3}$ at a temperature of 2300 K. The radiative Intensity is the directional radiative heat flux in $\mathrm{W/sr/m^2}$.

The intensity is obtained by the solution of the 1D radiation transport problem:

$$\frac{\mathrm{d}I}{\mathrm{d}s} = -\alpha I + e \tag{8}$$

which leads to:

$$I = \frac{e}{\alpha} \left(1 - \exp(-\alpha L)\right) \tag{9}$$

The maximum possible intensity is the black body limit of $\pi \sigma T^4$.

The results in figure 5 show that the radiative intensity increases with decreasing particle size and increasing soot mass fraction. The radiation is in a regime with significant self-absorption and at the present conditions the total radiative heat flux in the subsequent 3D analyses is expected to be sensitive to the assumptions of particle size and mass fraction.

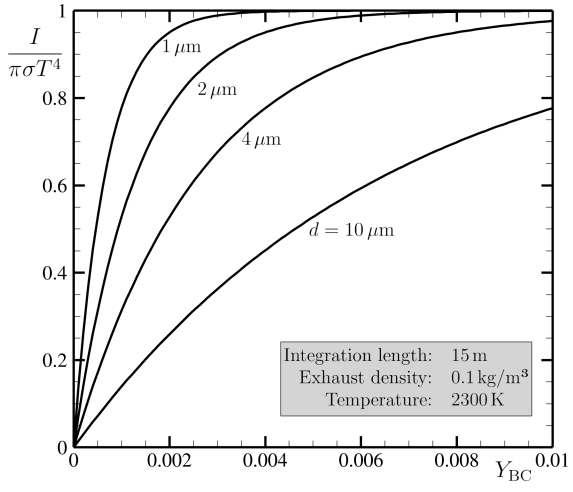

Fig. 3. Qualitative sensitivity analysis of the radiative intensity to particle size and mass fraction

6. RESULTS

A set of 3D radiation transfer computation using the Monte-Carlo-Method described in section 2 with the absorption and emission properties from section 5 was performed for the 3 trajectory points in table 1. The resulting radiative properties in the exhaust plume are depicted in figure 4. The distribution of the absorption coefficient is only shown for the first

trajectory point at the lowest altitude and reaches a maximum of 0.2 1/m in the core jet. Hence, the mean free path of the photons is around 5 m which is smaller than the characteristic length of the plume resulting in strong self-absorption of the radiation. The plume emissivity decreases significantly with increasing altitude. The main reason is the decrease in temperature due to the increasing expansion of the jet downstream of the main nozzle exit. Further, this stronger expansion also causes a reduced number density of soot particles. The gas generator exhaust does not contribute to the total emission (low gas temperature) and acts only as an additional absorber. Figure 4 also shows the distribution of radiative heat loads on the aft fuselage. The highest heat flux occurs at the outer region of the base plate. This is due to the shading effect of the main thrust nozzle. The total heat flux level decreases with altitude. This is due to the reduced emissivity of the exhaust gas. Further, at high altitudes, the radial gradient of the surface heat flux on the base plate is reduced. This is due to the larger geometrical size of the radiating plume and the resulting reduction of the protective shading effect of the thrust nozzle.

A quantitative comparison of the incident radiative heat flux on the base plate at a radius of 1.1 m with flight test data [1] is shown in figure 5. Despite of the simple numerical model, strong agreement between flight and numerical data is observed. Both, the qualitative trend of heat flux reduction with altitude and the quantitative heat flux levels are well reproduced by the numerical data.

7. SUMMARY

We presented a computational methodology to quantify plume radiation caused by soot particles in rocket exhaust plumes. A Photon-Monte-Carlo-Method is used to solve the radiative transfer equation in 3D space. This approach accounts for self-absorption in the exhaust gas which is significant as the plume is close to the optically thick limit for full scale launcher configurations. The radiative properties such as the absorption coefficient (inverse mean free path of the photons) and the emissivity (emitted radiative power per volume and direction) are derived from estimates of the soot mass fraction and particle size. The plume shape and thermodynamic properties are taken from classical CFD analyses. The method is calibrated and assessed based on available flight data for a kerosene-fueled rocket engine at different altitudes. Strong agreement with flight data was achieved by using estimates for soot properties which are consistent with the current literature. This method can either be used to quantify radiative heat loads for a known distribution of particle properties in the plume or, inversely, to estimate the particle properties from known measurements of the plume radiation.

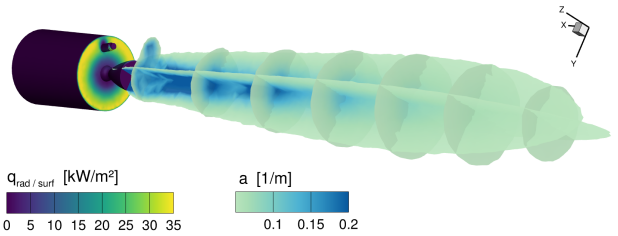

(a) TP1: absorption coefficient

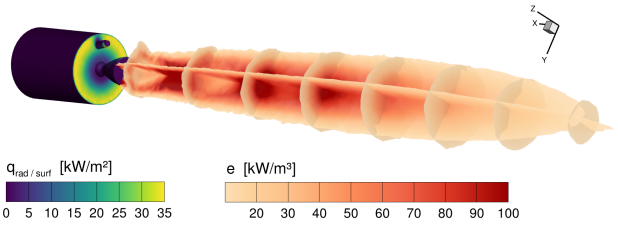

(b) TP1: emissivity

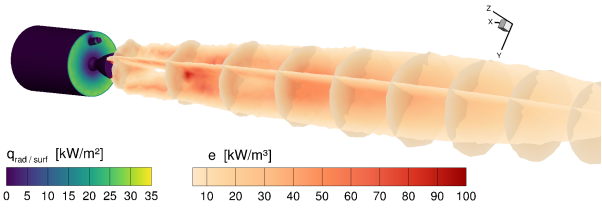

(c) TP2: emissivity

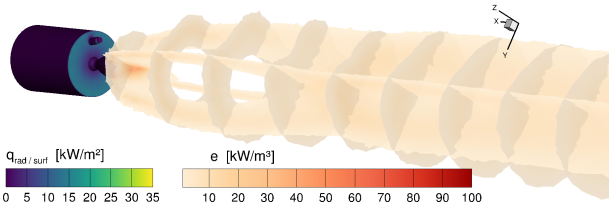

(d) TP3: emissivity

Fig. 4. Plume radative properties and base plate heat flux

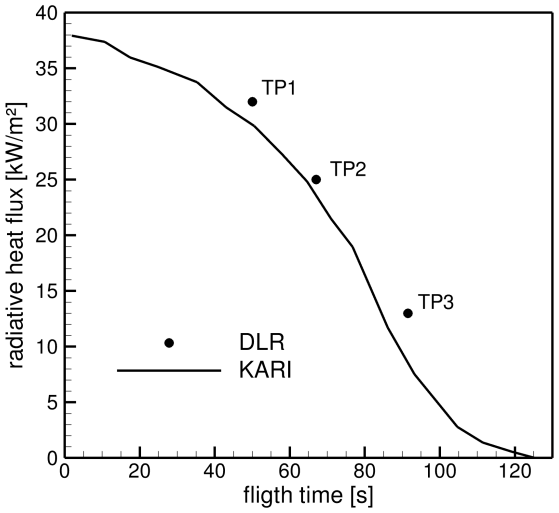

Fig. 5. Comparison to experimental data

8. REFERENCES

[1] Jongmin Kim, "Pre- and postflight thermal analysis of test launch vehicle fuselage," *Journal of Spacecraft and Rockets*, vol. 56, no. 6, pp. 1786–1794, 2019.

[2] W. J. Yang, H. Taniguch, and K. Kudo, "Radiative heat transfer by the monte carlo method," *Advances in Heat Transfer (Academic Press)*, vol. 27, pp. 1786–1794, 1995.

[3] D. Schwamborn, T. Gerhold, and R. Heinrich, "The dlr tau-code: recent applications in research and industry," in *ECCOMAS CFD 2006 CONFERENCE*, Kissimmee, Florida, Apr 2006.

[4] T. Ecker, S. Karl, and K. Hannemann, "Combustion modelling in solid rocket motor plumes," in *8th European Conference for Aeronautics and Space Sciences*. 2019, EUCASS.

[5] S. Gordon and B. J. McBride, "Computer Program for Calculation of Complex Chemical Equilibrium Compositions and Applications," Tech. Rep. NASA Reference Publication 1311, NASA, 1996.

[6] Lin Wang, Zhaohui Liu, Sheng Chen, and Chuguang Zheng, "Comparison of different global combustion mechanisms under hot and diluted oxidation conditions," *Combustion Science and Technology*, vol. 184, pp. 259–276, 02 2012.

[7] Doyoung Byun and Seung Wook Baek, "Numerical investigation of combustion with non-gray thermal radiation and soot formation effect in a liquid rocket engine," *International Journal of Heat and Mass Transfer*, vol. 50, no. 3, pp. 412–422, 2007.

[8] Y. Plastinin, G. F. Karabadzhak, B. Khmelinin, G. Baula, and A. Rodionov, "Determination of soot particle density and dimension in the lox/kerosene engine booster exhaust from remote measurements of radiation intensity," in *2nd International Conference on Green Propellants for Space Propulsion, Chia Laguna (Cagliari), Sardinia, Italy*, 2004.

[9] Juan David Blanco Camargo, *Literature review of the environmental impact on the atmosphere of rocket engine emissions during launch, flight and re-entry*, Master thesis, UNIVERSIDADE DE SÃO PAULO ESCOLA DE ENGENHARIA DE SÃO CARLOS, 2022.

[10] Martin Ross, Michael Mills, and Darin Toohey, "Potential climate impact of black carbon emitted by rockets," *Geophysical Research Letters*, vol. 37, no. 24, 2010.